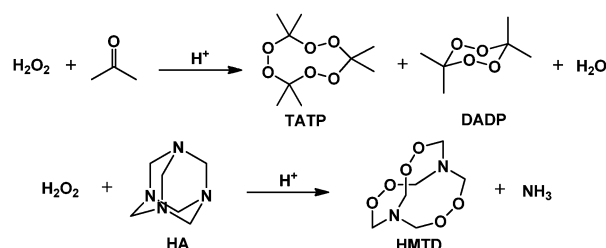# ChemComm

Differentiation among peroxide explosives with an optoelectronic nose†

Zheng Li, Will P. Bassett, Jon R. Askim and Kenneth S. Suslick*

Forensic identification of batches of homemade explosives (HME) poses a difficult analytical challenge. Differentiation among peroxide explosives is reported herein using a colorimetric sensor array and handheld scanner with a field-appropriate sampling protocol. Clear discrimination was demonstrated among twelve peroxide samples prepared from different reagents, with a classification accuracy > 98%.

There is an increasingly urgent need for rapid and highly selective detection of explosives, for both civilian and military security.[1,2] The ready production of homemade explosives (HMEs) and improvised explosive devices (IEDs) has become an increasing problem. Forensic identification of the source of production of HMEs poses a difficult analytical challenge, especially for in-field evaluations. Peroxide explosives, most notably triacetone triperoxide (TATP) and hexamethylene triperoxide diamine (HMTD), have not been extensively employed as mainstream military explosives due to their high sensitivity to impact, friction and static discharge.[3–6] Their ease of synthesis (Scheme 1) and difficulty of detection, however, make them explosives of choice for terrorists: both TATP and HMTD can be prepared from readily available starting materials (*i.e.*, hydrogen peroxide, an acid catalyst, and acetone for TATP or hexamethylene-tetramine for HMTD).[7,8]

Peroxide explosives such as TATP or HMTD are undetectable through direct fluorescent approaches (having no chromophores) and relatively difficult to detect by standard ion mobility spectrometers.[9,10] As a consequence, a large number of detection methods for TATP or HMTD have been developed in the past few years, most of which demand complex instrumentation, including electrochemical,[11,12] indirect fluorescence,[6,13–16] and mass spectrometry.[5,17–21] Examples of readily portable detection

Department of Chemistry, University of Illinois at Urbana-Champaign,
600 S. Mathews Ave., Urbana, Illinois 61801, USA. E-mail: ksuslick@illinois.edu
† Electronic supplementary information (ESI) available: Experimental protocol, supplementary figures and additional spectroscopic data. See DOI: 10.1039/c5cc06221g

Scheme 1   Reactions for the synthesis of TATP and HMTD.

methods for field detection of peroxides, however, remain limited and generally require destructive sampling.[22,23] Importantly, a handheld sensor, FIDO-Paxpoint,[24] has been used very recently in US international airports for peroxide detection.

The optoelectronic nose,[25–27] which uses digital imaging of colorimetric sensor arrays, has emerged as a powerful tool to discriminate and fingerprint both single analytes[28–31] and complex mixtures.[32–34] Colorimetric sensor arrays make use of a set of diverse chemoresponsive colorants whose color changes are determined by interactions with analytes; these interactions include redox, polarity, Brønsted and Lewis acid–base, and π–π interactions.[27,29,30]

Our group has previously reported the use of an acid catalyst combined with a colorimetric sensor array for the detection of TATP vapors with the detection limit as low as 2 ppb.[35] Recently, we have successfully developed a portable handheld reader for colorimetric sensor arrays.[36] In this work, we report the use of a handheld reader and a simple colorimetric sensor array, using a field-ready sampling protocol, for the forensic identification of peroxide HMEs and the differentiation of HMEs based on their synthetic preparation.

One of the analytical challenges for identification of HMEs remains their inherent lack of purity. HMEs generally contain variable amounts of impurities that reflect the protocol used for their synthesis and the nearly universal lack of post-synthetic purification. Especially for peroxide based energetic materials, there is no unified standard on the preparation of these unconventional explosives, and different synthetic procedures
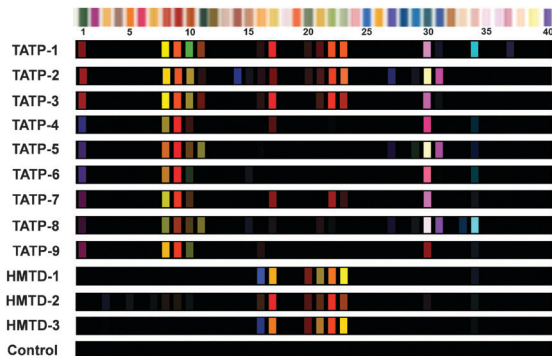
Fig. 1 Scaled difference maps of the 40-element colorimetric sensor array showing signal-to-noise (S/N) of nine TATP and three HMTD and a control. S/N ratios of 3–10 were scaled for display on an 8-bit RGB color scale (*i.e.*, 0–255).

(*e.g.*, H_2SO_4 or HNO_3 instead of HCl as the acid catalyst for TATP, Scheme 1) give rise to significantly different product mixtures.[7] In addition, trimetric TATP is known to degrade into its dimeric form, diacetone diperoxide (DADP), which may also lead to inconsistent sensing results.[37] To test the optoelectronic nose, we have examined the response of a colorimetric sensor array for the identification of nine separately synthesized samples of TATP and three of HMTD (Scheme 1 and Table 1) through the direct sampling of the saturated vapors from the solid explosives.

The colorimetric sensors used in this study are chemically diverse (see ESI,† Table S1); while this array has been optimized for oxidant detection, it still retains both Lewis and Brønsted acid/base responsive dyes and solvatochromic dyes. The sensors are mostly dosimetric (*i.e.*, essentially irreversible to peroxide exposure) in their response to oxidants. New sensors include ones that use Fenton reagent chemistry (Fe(II) catalysed production of strong radical oxidants) to cause color changes, other generic redox-sensitive dyes (tolidine, o-dianisidine, *etc.*), and hydrazines (*i.e.*, dinitrophenylhydrazine) for the specific detection of ketones or aldehydes (*e.g.*, from degradation products of TATP).

Several milligrams of each HME were tested using disposable 40-element colorimetric sensor arrays with a field-appropriate sampling protocol (see ESI† for further details); response to each

analyte sample was collected in quintuplicate trials. The scaled color difference maps of the sensor arrays after exposure to fresh TATP or HMTD samples (stored at 0 °C for one day after synthesis) are shown in Fig. 1.

Distinctive patterns in the color difference maps show that TATP interacts with sensor spots that contain redox dyes, diphenylhydrazine-containing dyes, and acid-sensitive pH indicators. Both TATP and especially H_2O_2 impurities will react with the redox dyes; acetone impurities or decomposition products from TATP react with the diphenylhydrazine dyes; acidic volatiles in the TATP vapor (which are attributed to the acid inclusion within the solid crystals)[38] provide for pH indicators' responses.

The differences in the array responses to TATP samples prepared from different peroxide sources can be differentiated even by eye by comparing the response of Fe(II)-containing redox spots (Spot 1 and 11). TATP preparations using different acids are also readily separable from one another based on their different responses to pH indicators (Spot 17, 20–23 and 30–31); for example, samples prepared using H_2SO_4 give a higher signal than those prepared with HCl or HNO_3, likely due to greater loss of the more-volatile acids during preparation.

Interestingly, the array response to HMTD does not involve the redox indicators. Vapor pressure of HMTD is calculated to be <0.04 Pa,[39] less than 1% of TATP or DADP[40] under the experimental conditions (*i.e.*, room temperature), which explains the lack of detectable volatile oxidants. Observed signals come purely from the degradation products and impurities in the sample; the samples show response only among base-sensitive and neutral pH indicators (Spot 16–17, 20–23), which illustrates the basic nature of sample impurities (*e.g.*, trimethylamine (TMA) and hexamethylenetetramine (hexamine, HA)). The overall response depends on the rigor of purification procedures; a purification protocol for products is therefore provided in the ESI† (see Fig. S3 in ESI†).

A model-free statistical approach, hierarchical cluster analysis (HCA),[41–43] was used to evaluate the discriminatory ability of the sensor array. The resulting dendrogram is shown in Fig. 2;

Table 1 Synthesis of TATP and HMTD: nine TATP and three HMTD formulations

Sample	Reactants	Acid catalyst
TATP-1	$(CH_3)_2CO + H_2O_2$	HCl
TATP-2	$(CH_3)_2CO + H_2O_2$	H_2SO_4
TATP-3	$(CH_3)_2CO + H_2O_2$	HNO_3
TATP-4	$(CH_3)_2CO + Na_2CO_3·1.5H_2O_2$	HCl
TATP-5	$(CH_3)_2CO + Na_2CO_3·1.5H_2O_2$	H_2SO_4
TATP-6	$(CH_3)_2CO + Na_2CO_3·1.5H_2O_2$	HNO_3
TATP-7	$(CH_3)_2CO + CO(NH_2)_2·H_2O_2$	HCl
TATP-8	$(CH_3)_2CO + CO(NH_2)_2·H_2O_2$	H_2SO_4
TATP-9	$(CH_3)_2CO + CO(NH_2)_2·H_2O_2$	HNO_3
HMTD-1	$(CH_2)_6N_4 + H_2O_2$	Citric acid
HMTD-2	Fuel cubes + H_2O_2	Citric acid
HMTD-3	$HCHO + NH_3 + H_2O_2$	Citric acid

H_2O_2: 30 wt% aqueous solution; HCHO: ~37 wt% aqueous solution; NH_3: ~29 wt% aqueous solution.
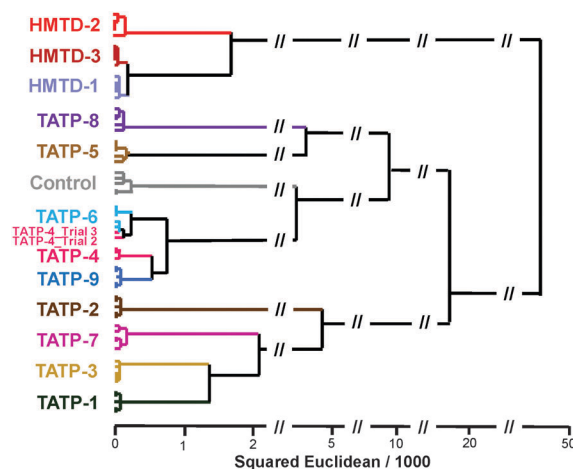

Fig. 2 Hierarchical cluster analysis (HCA) dendrogram of twelve peroxide explosives tested at the bulk sample size of 10 mg and a control out of 65 trials. All species were clearly discriminable against each other except for two trials from TATP-4 that were misclassified with TATP-6.
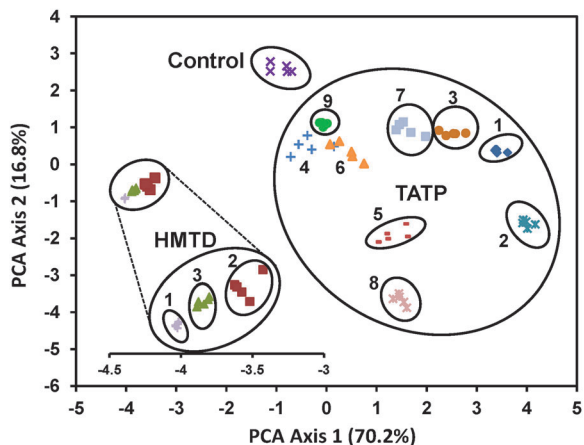
Fig. 3 Two-dimensional principal components analysis plot for quintuplicate trials of twelve preparations of peroxide explosives (number nearby each cluster represents the sample label of each corresponding peroxide) and a control; $n = 65$. Misclassification was only observed between TATP-4 and TATP-6.

Table 2 Purity of nine TATP and three HMTD samples from headspace analysis

	[TATP]/([TATP] + [DADP])^a (%)	
Sample	Fresh (1 d)	Aged (30 d)
TATP-1	79.2	35.8
TATP-2	69.0	47.6
TATP-3	66.2	45.5
TATP-4	99.1	96.5
TATP-5	98.4	96.7
TATP-6	96.3	93.9
TATP-7	95.9	54.1
TATP-8	96.5	53.3
TATP-9	96.7	57.7

	[HMTD]/([TMA] + [HA] + [HMTD])^a (%)	
Sample	Fresh (1 d)	Aged (30 d)
HMTD-1	87.5	84.3
HMTD-2	88.6	82.9
HMTD-3	85.9	81.6

^{a} Calculated from integrated peak areas. TMA, trimethylamine; HA, hexamine.

all analytes are represented by quintuplicate trials. The HCA dendrogram shows perfect discrimination among all the analytes with the exception of two confusions between TATP-4 and TATP-6; this confusion is not unexpected, given that these two samples of TATP were prepared in a very similar manner: mixing acetone, sodium percarbonate with a volatile acid (HCl or HNO$_3$, respectively). The effects of aging of TATP and HMTD samples were also examined and only minimally effected the sensor array response (see ESI,† Fig. S4 and S5), in spite of significant structural changes in crystal morphology (see ESI,† Fig. S6).

Principal component analysis (PCA)[43,44] was performed to provide a measure of the dimensionality of the data. Given the very limited range of chemical diversity present among these analytes, relatively low dimensionality was expected and indeed observed: two dimensions account for 87% of the total variance and five dimensions are required to capture 95% of the variance (ESI,† Fig. S7). A score plot of the first two principal components (Fig. 3) shows relatively good separation among the analytes, as indicated by circling obvious clusters. All three HMTD samples were separable from TATP, and all the TATP (except TATP-4 and TATP-6) were differentiable.

A more robust and supervised classification method, support vector machine (SVM) analysis, was used to create optimized classifiers using LIBSVM, an open-source SVM library.[26] SVM results using a leave-one-out permutation method are shown in Table S2 (see ESI†). Using SVM analysis, no errors in classification were found including all TATP samples, i.e., the error rate of predictive classification is <1.5%.

GC-MS analyses were conducted to understand the chemical composition of freshly prepared peroxides and their possible degradation during aging. Headspace volatiles were sampled using solid-phase microextraction (SPME) in a protocol which closely matched the sampling condition using handheld device. The compositions of TATP and HMTD samples as determined by SPME GC-MS are given in Table 2. TATP prepared from H$_2$O$_2$ have relatively high levels of DADP for

both fresh and aged samples, and aging for 30 days yields more dimeric product DADP (see ESI,† Fig. S8 and Table S3). Fresh TATP samples prepared from percarbonate or urea peroxide are nearly pure TATP; upon aging, however, TATP prepared from urea peroxide shows a considerable amount of DADP, while TATP synthesized from percarbonate appears to have higher stability and longer shelf-life than the other TATP samples (see ESI,† Table S3). Though HMTD is much less volatile than TATP, SPME GC spectra still detect the degradation products TMA and HA (see ESI,† Fig. S8), which are primarily responsible for the sensor array responses. Good crystallinity of both TATP and HMTD samples was observed and discussed in ESI,† Fig. S8.

The limits of detection (LOD) in sample size for the bulk peroxide explosives were examined. The LOD is defined as the sample amount determined by extrapolation that provides a signal (i.e., the overall response to an analyte) at least three times as great as the noise (i.e., the standard deviation among blank controls). In general, LODs for analytes scale with volatility: higher volatility leads to greater colorimetric array response; the reactivity of the volatiles, however, also plays a critical role in array response. For three representative analytes (two TATP and one HMTD), we plotted the array response as a function of sample amount ranging from 1 to 10 mg (see ESI,† Fig. S9). Based on the extrapolated calibration curve, the LODs for three typical explosives are all determined to be at μg level: ~90 μg for TATP-1, ~140 μg for TATP-5 and ~120 μg for HMTD-1. We emphasize that these sensor arrays are not intended for trace detection of explosives, but rather for forensic identification of the method of manufacture of a discovered HME or IED; in real world situations, intelligence information as to the explosive maker can be extremely valuable.

In field work, it is probable that there will be other odorants present in the air sampled that could potentially interfere with identification of the targeted analytes. In order to gauge the specificity of the sensor array, we examined sensor array response to 10 mg of five possible interferents that are common

in an airport atmosphere[45] (toothpaste, sunscreen, lipstick, perfume and eye drops) as a comparison to the positive responses from two peroxides (TATP-1 and HMTD-1), as provided in ESI,† Fig. S10. These five interferents give easily distinguishable responses from the peroxide explosives and are totally separable from the peroxides. In addition, as we have previously demonstrated,[28–31] the colorimetric sensor array is very insensitive to changes in ambient humidity.

In conclusion, we have developed a colorimetric sensor array that can detect and discriminate among peroxide explosives based on their source or manufacturing details. TATP vapors undergo acid-catalysed decomposition that release detectable volatiles while the much less volatile HMTD contains detectable volatile basic impurities. Hierarchical cluster analysis, principal component analysis, and support vector machine analysis show excellent discrimination among peroxide explosives produced by a range of synthetic methods. Aging over 30 days did not affect the results, even though aging does alter the constituent and crystalline phase of TATP as confirmed by GC-MS and PXRD tests. Detection limits for both peroxides are calculated to be $\sim$100 µg. This method has significant implications in peroxide explosives identification and may prove to be a useful supplement to other available detecting technologies used in security checks and forensic evaluation of improvised explosives.

Notes and references

1 S. Meyer, *Sci. Secure J. Biotechnol.*, 2012, **25**, 309–325.
2 J. Yinon, *Counterterrorist Detection Techniques of Explosives*, Elsevier, B. V., Amsterdam, 2007.
3 A. C. T. Duin, Y. Zeiri, F. Dubnikova, R. Kosloff and W. A. Goddard, *J. Am. Chem. Soc.*, 2005, **127**, 11053–11062.
4 J. C. Oxley, J. L. Smith, P. R. Bowden and R. C. Rettinger, *Propellants, Explos., Pyrotech.*, 2013, **38**, 244–254.
5 P. F. Wilson, B. J. Prince and M. J. McEwan, *Anal. Chem.*, 2006, **78**, 575–579.
6 S. Parajuli and W. Miao, *Anal. Chem.*, 2013, **85**, 8008–8015.
7 G. R. Peterson, W. P. Bassett, B. L. Weeks and L. J. Hope-Weeks, *Cryst. Growth Des.*, 2013, **13**, 2307–2311.
8 F. Dubnikova, R. Kosloff, J. Almog, Y. Zeiri, R. Boese, H. Itzhaky, A. Alt and E. Keinan, *J. Am. Chem. Soc.*, 2005, **127**, 1146–1159.
9 S. Eren, A. Uzer, Z. Can, T. Kapudan, E. Ercag and R. Apak, *Analyst*, 2010, **135**, 2085–2091.
10 R. Burks and D. Hage, *Anal. Bioanal. Chem.*, 2009, **395**, 301–313.
11 D. F. Laine and I. F. Cheng, *Microchem. J.*, 2009, **91**, 125–128.
12 R. A. A. Munoz, D. Lu, A. Cagan and J. Wang, *Analyst*, 2007, **132**, 560–565.
13 L. Chen, Y. Gao, Y. Fu, D. Zhu, Q. He, H. Cao and J. Cheng, *RSC Adv.*, 2015, **5**, 29624–29630.
14 C. He, D. Zhu, Q. He, L. Shi, Y. Fu, D. Wen, H. Cao and J. Cheng, *Chem. Commun.*, 2012, **48**, 5739–5741.
15 S. W. Thomas, G. D. Joly and T. M. Swager, *Chem. Rev.*, 2007, **107**, 1339–1386.
16 S. Malashikhin and N. S. Finney, *J. Am. Chem. Soc.*, 2008, **130**, 12846–12847.
17 T. P. Forbes and E. Sisco, *Anal. Chem.*, 2014, **86**, 7788–7797.
18 I. Cotte-Rodriguez, H. Chen and R. G. Cooks, *Chem. Commun.*, 2006, 953–955, DOI: 10.1039/B515122H.
19 S.-H. Wu, J.-H. Chi, Y.-T. Wu, Y.-H. Huang, F.-J. Chu, J.-J. Horng, C.-M. Shu and J.-C. Charpentier, *J. Loss Prev. Process Ind.*, 2012, **25**, 1069–1074.
20 A. Crowson and M. S. Beardah, *Analyst*, 2001, **126**, 1689–1693.
21 W. Fan, M. Young, J. Canino, J. Smith, J. Oxley and J. Almirall, *Anal. Bioanal. Chem.*, 2012, **403**, 401–408.
22 M. O. Salles, G. N. Meloni, W. R. de Araujo and T. R. L. C. Paixao, *Anal. Methods*, 2014, **6**, 2047–2052.
23 J. Chen, W. Wu and A. J. McNeil, *Chem. Commun.*, 2012, **48**, 7310–7312.
24 R. Deans, A. Rose, K. M. Bardon, L. F. Hancock and T. M. Swager, *US Pat.*, 7,799,573, 2010.
25 N. A. Rakow and K. S. Suslick, *Nature*, 2000, **406**, 710–713.
26 K. S. Suslick, *MRS Bull.*, 2004, **29**, 720–725.
27 J. R. Askim, M. Mahmoudi and K. S. Suslick, *Chem. Soc. Rev.*, 2013, **42**, 8649–8682.
28 N. A. Rakow, A. Sen, M. C. Janzen, J. B. Ponder and K. S. Suslick, *Angew. Chem., Int. Ed.*, 2005, **44**, 4528–4532.
29 M. C. Janzen, J. B. Ponder, D. P. Bailey, C. K. Ingison and K. S. Suslick, *Anal. Chem.*, 2006, **78**, 3591–3600.
30 S. H. Lim, L. Feng, J. W. Kemling, C. J. Musto and K. S. Suslick, *Nat. Chem.*, 2009, **1**, 562–567.
31 L. Feng, C. J. Musto, J. W. Kemling, S. H. Lim, W. Zhong and K. S. Suslick, *Anal. Chem.*, 2010, **82**, 9433–9440.
32 B. A. Suslick, L. Feng and K. S. Suslick, *Anal. Chem.*, 2010, **82**, 2067–2073.
33 J. R. Carey, K. S. Suslick, K. I. Hulkower, J. A. Imlay, K. R. C. Imlay, C. K. Ingison, J. B. Ponder, A. Sen and A. E. Wittrig, *J. Am. Chem. Soc.*, 2011, **133**, 7571–7576.
34 Y. Zhang, J. R. Askim, W. Zhong, P. Orlean and K. S. Suslick, *Analyst*, 2014, **139**, 1922–1928.
35 H. Lin and K. S. Suslick, *J. Am. Chem. Soc.*, 2010, **132**, 15519–15521.
36 J. R. Askim and K. S. Suslick, *Anal. Chem.*, 2015, **87**, 7810–7816.
37 M. Fitzgerald and D. Bilusich, *J. Forensic Sci.*, 2011, **56**, 1143–1149.
38 J. C. Oxley, J. L. Smith and H. Chen, *Propellants, Explos., Pyrotech.*, 2002, **27**, 209–216.
39 P. L. Damour, A. Freedman and J. Wormhoudt, *Propellants, Explos., Pyrotech.*, 2010, **35**, 514–520.
40 J. C. Oxley, J. L. Smith, W. Luo and J. Brady, *Propellants, Explos., Pyrotech.*, 2009, **34**, 539–543.
41 J. Janata, *Principles of Chemical Sensors*, Springer, New York, 2nd edn, 2009.
42 J. F. Hair, B. Black, B. Babin, R. E. Anderson and R. L. Tatham, *Multivariate Data Analysis*, Prentice Hall, New York, 6th edn, 2005.
43 R. A. Johnson and D. W. Wichern, *Applied Multivariate Statistical Analysis*, Prentice Hall, New York, 6th edn, 2007.
44 I. T. Jolliffe, *Principal Component Analysis*, Springer, New York, 2002.
45 D. Gopalakrishnan and W. R. Dichtel, *J. Am. Chem. Soc.*, 2013, **135**, 8357–8362.